The Harper–Hofstadter Hamiltonian and conical diffraction in photonic lattices with grating assisted tunneling

Dubček, Tena; Lelas, Karlo; Jukić, Dario; Pezer, Robert; Soljačić, Marin; Buljan, Hrvoje

New Journal of Physics
The open access journal at the forefront of physics

Deutsche Physikalische Gesellschaft DPG
IOP Institute of Physics

Published in partnership with: Deutsche Physikalische Gesellschaft and the Institute of Physics

CrossMark

OPEN ACCESS

RECEIVED
25 August 2015

ACCEPTED FOR PUBLICATION
5 November 2015

PUBLISHED
7 December 2015

PAPER

The Harper–Hofstadter Hamiltonian and conical diffraction in photonic lattices with grating assisted tunneling

Tena Dubček[1], Karlo Lelas[2], Dario Jukić[1,3], Robert Pezer[4], Marin Soljačić[5] and Hrvoje Buljan[1]

[1] Department of Physics, University of Zagreb, Bijenička c. 32, 10000 Zagreb, Croatia
[2] Faculty of Textile Technology, University of Zagreb, Prilaz baruna Filipovića 28a, 10000 Zagreb, Croatia
[3] Max Planck Institute for the Physics of Complex Systems, Nöthnitzer Str. 38, 01187 Dresden, Germany
[4] Faculty of Metallurgy, University of Zagreb, Aleja narodnih heroja 3, HR 44 103 Sisak, Croatia
[5] Department of Physics, Massachusetts Institute of Technology, Cambridge, MA 02139, USA

E-mail: hbuljan@phy.hr

Keywords: synthetic magnetic fields, photonic lattices, topological effects, conical diffraction

Abstract

We propose the realization of a grating assisted tunneling scheme for tunable synthetic magnetic fields in optically induced one- and two-dimensional dielectric photonic lattices. As a signature of the synthetic magnetic fields, we demonstrate conical diffraction patterns in particular realization of these lattices, which possess Dirac points in k-space. We compare the light propagation in these realistic (continuous) systems with the evolution in discrete models representing the Harper–Hofstadter Hamiltonian, and obtain excellent agreement.

1. Introduction

Synthetic magnetism for photons is a unique tool for the manipulation and control of light, and for the design of novel topological phases and states in photonics [1–18]. Topological photonics is a rapidly growing field [18], advancing in parallel to analogous efforts in ultracold atomic gases [19, 20], inspired by the development of topological insulators in condensed matter physics [21]. One motivating aspect of topological photonic systems is the existence of unidirectional backscattering immune states [1–4], which are robust to imperfections, and thus may serve as novel waveguides and for building integrated photonic devices. The first experimental observations of such edge states were in the microwave domain, in magneto-optical photonic crystals [4], theoretically proposed in [1–3]. In the optical domain, imaging of topological edge states was reported in Floquet topological insulators, implemented in modulated honeycomb photonic lattices [5], and in the two-dimensional array of coupled optical-ring resonators [6]. The strategies for obtaining synthetic magnetic/gauge fields and topological phases for optical photons are closely related to the system at hand. In systems of coupled optical resonators, the strategy is to tune the phase of the tunneling between coupled cavities [6–9]; for example, by using link resonators of different length [6, 7], by time-modulation of the coupling [9] or the resonant frequencies of the cavities [14]. Photonic topological insulators were also proposed in superlattices of metamaterials with strong magneto-electric coupling [15]. In 2D photonic lattices (waveguide arrays), pseudomagnetic fields have been demonstrated by inducing 'strain' in optical graphene [10]. Lattice modulation has also been shown to be a fruitful approach in these systems [11–14, 17]. By modulating 1D photonic lattices along the propagation axis, one can choose the sign of the hopping parameter between neighbouring sites, as was realized in a system with alternating positive and negative couplings and resulted in 1D conical diffraction [11]. Transversely modulated waveguide arrays were proposed for the realization of the nonlinear Harper model [12], whereas topological states were achieved in 1D photonic quasicrystals [13]. Moreover, optical analogues of the so called laser assisted tunneling in atomic systems were suggested for creating synthetic magnetic fields in discrete square lattices [14] and recently experimentally studied in laser-fabricated photonic Wannier–Stark ladders [17].

However, all of the above mentioned photonic lattices are in reality continuous dielectric structures. An important test of the viability of a method considered for producing synthetic magnetism is the comparison of

light propagation in a continuous system with the propagation in the corresponding discrete model. Here, we propose the realization of a grating assisted tunneling scheme for tunable synthetic magnetic fields in optically induced one- and two-dimensional dielectric photonic lattices [22–26]. As a signature of the synthetic magnetic fields, we demonstrate conical diffraction patterns in particular realization of these lattices, which possess Dirac points in k-space. We compare the light propagation in these realistic (continuous) systems with the evolution in discrete models representing the Harper–Hofstadter Hamiltonian [31, 32], and obtain excellent agreement.

Methods encountered in photonics are sometimes closely related to methods in other branches of physics. For example, synthetic magnetic fields were created by using 'strain' in optical graphene [10], analogously to the scheme with strained real graphene [28]. Furthermore, many of the results obtained with ultracold atoms are viable in photonics, and perhaps even more of them are feasible, because heating by spontaneous emission, which is present in ultracold atomic systems, is absent in photonic systems. The method we consider is analogous to those used in [14, 17]; however, instead of using curved laser written waveguides [14, 17, 29] to create an effective linear tilt of the index of refraction, here we propose to use the optical induction technique and/or a temperature gradient, as elaborated below. All these schemes were inspired by the so called laser assisted tunneling scheme that was implemented in optical lattices with ultracold atoms [33–35]. Laser assisted tunneling is based on theoretical proposals in [36, 37], subsequently developed to experimentally realize the Harper–Hofstadter Hamiltonian [34, 35], and staggered magnetic fields in optical superlattices [33].

Historically, the first synthetic magnetic fields were implemented in rapidly rotating Bose–Einstein condensates (BECs) by using the Coriolis force to mimick the magnetic Lorentz force [38, 39], whereas the first implementation based on laser-atom interactions used spatially dependent Raman optical coupling between internal hyperfine atomic states in bulk BECs [40]. The latter scheme used the analogy between the Aharonov–Bohm and the Berry phase [19, 20]. Beside the schemes with laser assisted tunneling [33–35], methods yielding synthetic magnetism in optical lattices include shaking of the optical lattice [41] and an all-optical scheme which enables flux rectification in optical superlattices [42]. For detailed reviews on synthetic gauge fields and potentials in cold atoms see [19, 20].

2. Results

2.1. The photonic system

We consider the paraxial propagation of light in a photonic lattice defined by the index of refraction $n = n_0 + \delta n(x, y, z)$ ($\delta n \ll n_0$), where n_0 is the constant background index of refraction, and $\delta n(x, y, z)$ describes small spatial variations, which are slow along the propagation z-axis. The slowly varying amplitude of the electric field $\psi(x, y, z)$ follows the (continuous) Schrödinger equation [26]:

$$\mathrm{i}\frac{\partial\psi}{\partial z} = -\frac{1}{2k}\nabla^2\psi - \frac{k\delta n}{n_0}\psi; \tag{1}$$

here, $\nabla^2 = \partial^2/\partial x^2 + \partial^2/\partial y^2$, and $k = 2\pi n_0/\lambda$, where λ is the wavelength in vacuum. From now on we will refer to $\delta n(x, y, z)$ as the potential or index of refraction. In the simulations we use $n_0 = 2.3$, corresponding to the systems that were used to implement the optical induction technique [23, 24], and $\lambda = 500$ nm.

2.2. Grating assisted tunneling and conical diffraction

For clarity, let us first present the grating assisted tunneling method in a 1D photonic lattice. If the potential is a periodic lattice, $\delta n_{\mathrm{L}}(x) = \delta n_{\mathrm{L}}(x + a)$, where a is the lattice constant, and if the lattice is sufficiently 'deep', the propagation of light can be approximated by using a discrete Schrödinger equation [26, 43]:

$$\mathrm{i}\frac{\mathrm{d}\psi_m}{\mathrm{d}z} = -\left(J_x\psi_{m-1} + J_x\psi_{m+1}\right), \tag{2}$$

where J_x quantifies the tunneling between adjacent waveguides and $\psi_m(z)$ is the amplitude at the mth lattice site, i.e., waveguide. To create a synthetic magnetic field, here we use the strategy to tune the phase of the tunneling between lattice sites. For this 1D lattice, we seek a scheme which effectively renormalizes J_x to get $K_x \exp(\mathrm{i}\phi_m)$, where ϕ_m denotes the phase for tunneling from site m to site $m + 1$. The scheme is illustrated in figure 1. In figure 1(a) we show the potential $\delta n(x, z)$, which can be modeled as a discrete lattice with complex tunneling parameters $K_x \exp(\mathrm{i}\phi_m)$ shown in figure 1(b).

Let us gradually present this method wherein the index of refraction is varied as in figure 1(a). In figure 1(e), we show the propagation of intensity in a continuous 1D model in the lattice potential $\delta n_{\mathrm{L}}(x) = \delta n_{\mathrm{L}0}\cos^2(\pi x/a)$, with $\psi(x, 0) = \sqrt{I}\mathrm{e}^{-x^2/(3a)^2}$; $\delta n_{\mathrm{L}0} = 4 \times 10^{-4}$, $a = 10$ μm. We see the usual diffraction pattern for a spatially broad excitation covering several lattice sites [26]. Next, suppose that we introduce a linear gradient of index of refraction along the x-direction $\delta n_{\mathrm{T}}(x) = -\eta x$ in addition to the lattice potential, such that $\delta n = \delta n_{\mathrm{L}}(x) + \delta n_{\mathrm{T}}(x)$. For a sufficiently large tilt, the tunneling is *suppressed*. This can be seen from

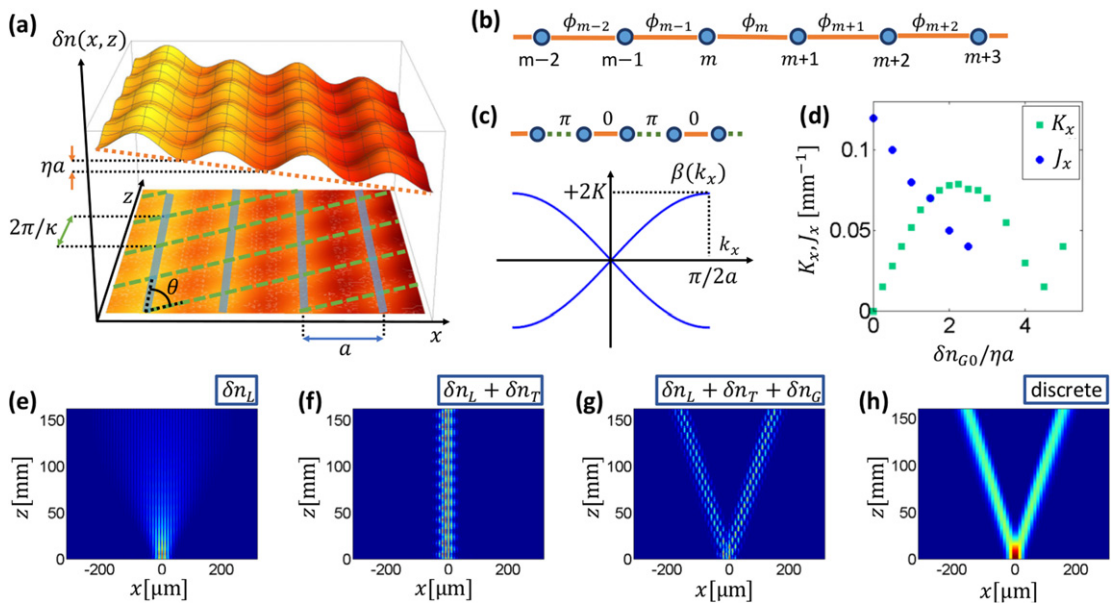

Figure 1. Illustration of the grating assisted tunneling scheme. (a) Sketch of the spatial dependence of the index of refraction $\delta n_{\mathrm{L}}(x, z) = \delta n_{\mathrm{L}} + \delta n_{\mathrm{T}} + \delta n_{\mathrm{G}}$, which creates a synthetic magnetic field in a photonic lattice. A 1D photonic lattice ($\delta n_{\mathrm{L}} = \delta n_{\mathrm{L0}} \cos^2(\pi x/a)$) is superimposed with a linear gradient index in the x direction ($\delta n_{\mathrm{T}} = -\eta x$, orange dotted line), and an additional small grating potential ($\delta n_{\mathrm{G}} = \delta n_{\mathrm{G0}} \cos^2((q_x x - \kappa z)/2)$), at a small angle ($\theta$ is on the order of 1°) with respect to the z axis. In the xz plane we plot the projection of δn_{L} (blue bold lines), and the grating (green dashed lines). (b) A discrete lattice with complex tunneling matrix elements between sites, $K_x \mathrm{e}^{\mathrm{i}\phi_m}$, and spatially dependent phases ϕ_m, can model the system in (a). (c) A particular choice of θ (see text), yields a lattice with $\phi_m = \pi m$, and a dispersion with a 1D Dirac cone at $k_x = 0$. (d) The amplitude of the tunneling K_x as a function of the strength of the grating δn_{G0} (green squares). The tunneling amplitude J_x versus δn_{G0} for a system without the tilt. (e)–(g) Numerical simulation of the evolution of a wavepacket that initially excites modes close to $k_x = 0$ in the continuous 1D photonic lattice. (e) Diffraction in a periodic photonic lattice δn_{L}. (f) Propagation in the tilted system, $\delta n_{\mathrm{L}} + \delta n_{\mathrm{T}}$, shows that the tunneling (diffraction) is suppressed. (g) The tunneling is restored by an additional grating potential with $q_x = \pi/a$. (h) Propagation of the wavepacket in the corresponding discrete model illustrated in (c).

figure 1(f) which shows the propagation of intensity in a tilted potential with $\eta = 0.1\ \delta n_{\mathrm{L0}}/a$; the tilt should be smaller than the gap between the first two bands. It should be noted that in the context of continuous periodic lattices with strong tilt, the suppression of tunneling can also be interpreted as Bloch oscillations with negligible amplitude. Finally, let us introduce an additional small grating potential at a small angle θ with respect to the z-axis, $\delta n_{\mathrm{G}}(x, z) = \delta n_{\mathrm{G0}} \cos^2((q_x x - \kappa z)/2)$, such that $\delta n(x, z) = \delta n_{\mathrm{L}}(x) + \delta n_{\mathrm{T}}(x) + \delta n_{\mathrm{G}}(x, z)$. This total potential $\delta n(x, z)$ is illustrated in figure 1(a). The 'frequency' κ is determined by the angle θ of the grating with respect to the z-axis, which is chosen such that $\kappa = \eta a k/n_0$ and the grating forms a z-dependent perturbation resonant with the index offset between neighboring lattice sites ηa (figure 1(a)). The grating *restores* the tunneling along the x-axis, hence the term *grating assisted tunneling*. Restored tunneling is seen in figure 1(g) which shows diffraction for identical initial conditions as in figures 1(e) and (f); the grating parameters are $q_x = \pi/a$ and $\delta n_{\mathrm{G0}} = 0.1\delta n_{\mathrm{L0}}$.

However, the diffraction pattern is drastically changed. In order to interpret it, we point out that, for resonant tunneling where $\kappa = \eta a k/n_0$ and a sufficiently large tilt ($J \ll \eta$), z-averaging over the rapidly oscillating terms shows that the system can be modeled by an effective discrete Schrödinger equation (e.g., see [34] for ultracold atoms):

$$\mathrm{i}\frac{\mathrm{d}\psi_m}{\mathrm{d}z} = -\left(K_x \mathrm{e}^{\mathrm{i}\phi_{m-1}}\psi_{m-1} + K_x \mathrm{e}^{-\mathrm{i}\phi_m}\psi_{m+1}\right), \tag{3}$$

where $\phi_m = \mathbf{q} \cdot \mathbf{R}_m = q_x m a$. In figure 1(g) we used $q_x = \pi/a$, i.e., $\phi_m = m\pi$. Such a discrete lattice is illustrated in figure 1(c); its dispersion having a 1D Dirac cone at $k_x = 0$. For a wavepacket that initially excites modes close to $k_x = 0$, the diffraction in the discrete model (3) yields the so-called (1D) conical diffraction pattern [11], as illustrated in figure 1(h). The initial conditions for propagation in the discrete model correspond to the initial conditions in the continuous system, $\psi_m(0) = \sqrt{I}\,\mathrm{e}^{-(m/3)^2}$, and $K_x = 0.053\ \mathrm{mm}^{-1}$. Thus, we interpret the diffraction pattern in figure 1(g) as 1D conical diffraction, a signature of the discrete model depicted in figure 1(c). A comparison of the discrete (figure 1(h)) and the realistic continuous model (figure 1(g)), clearly shows that we can use grating assisted tunneling to tune the phases of the tunneling parameters in the discrete Schrödinger equation, thereby realizing synthetic magnetic fields.

Before proceeding to 2D systems, we discuss the amplitude of the tunneling matrix elements K_x as a function of the strength of the grating δn_{G0}. Figure 1(d) shows K_x (green squares) and J_x (blue circles) versus δn_{G0}, where J_x

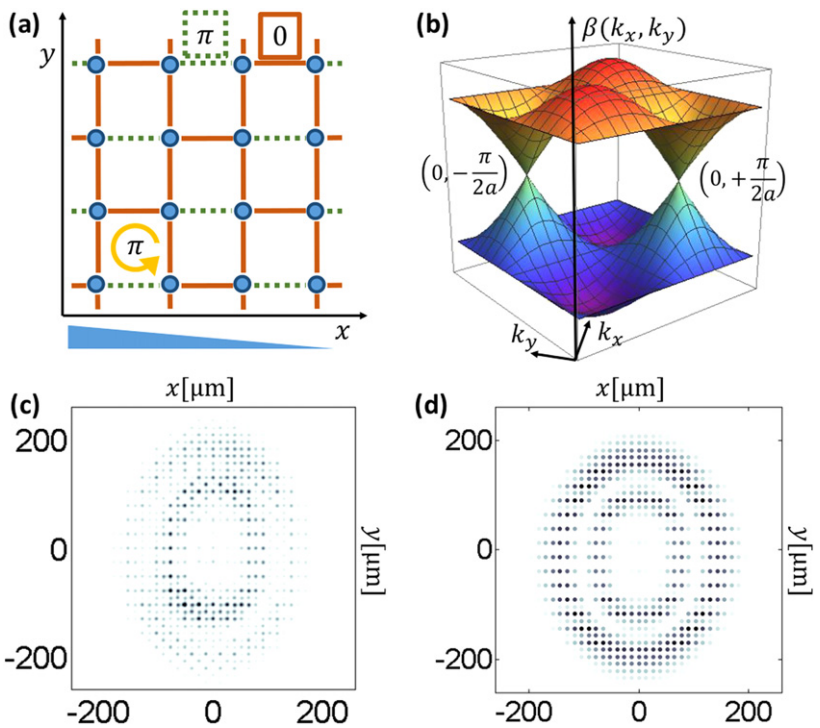

Figure 2. Grating assisted tunneling and conical diffraction in a square photonic lattice. (a) Sketch of the 2D lattice with grating assisted tunneling along the x-direction. The resulting nontrivial hopping phases π and 0 are denoted with dashed and solid lines, respectively. A wavepacket that makes one loop around the plaquette accumulates the phase π. (b) The lattice possesses two 2D Dirac cones at $(k_x, k_y) = (0, \pm\pi/2a)$ in the dispersion $\beta(k_x, k_y)$, where β is the propagation constant. (c) Intensity of a beam, which initially excites modes in the vicinity of the Dirac points, after propagation for $z = 162$ mm. The intensity has two concentric rings corresponding to the conical diffraction pattern. (d) Simulation of the diffraction pattern in the discrete model corresponding to the lattice in (a), which also exhibits conical diffraction (see text for details).

corresponds to the potential which includes the lattice and the grating, but no tilt. The amplitudes J_x and K_x are obtained by comparing the diffraction pattern of the discrete with the continuous model, and adjusting J_x and K_x until the two patterns coincide, as in figures 1(g) and (h). Our results in figure 1(d) are in agreement with those in ultracold atoms (e.g., see figure 3(a) in [34]).

The extension of the scheme to 2D lattices is straightforward. We consider a square lattice, $\delta n_{\mathrm{L}} = \delta n_{\mathrm{L0}}(\cos^2(\pi x/a) + \cos^2(\pi y/a))$, the tilt in the x-direction, $\delta n_{\mathrm{T}}(x) = -\eta x$, and the grating which has the form $\delta n_{\mathrm{G}}(x, y, z) = \delta n_{\mathrm{G0}} \cos^2((q_x x + q_y y - \kappa z)/2)$. Propagation of light in the total potential $\delta n(x, y, z) = \delta n_{\mathrm{L}}(x, y) + \delta n_{\mathrm{T}}(x) + \delta n_{\mathrm{G}}(x, y, z)$ can be modeled by the discrete Schrödinger equation (the derivation is equivalent to that in [34] for ultracold atoms):

$$\mathrm{i}\frac{\mathrm{d}\psi_{m,n}}{\mathrm{d}z} = -\Big(K_x \mathrm{e}^{\mathrm{i}\phi_{m-1,n}}\psi_{m-1,n} + K_x \mathrm{e}^{-\mathrm{i}\phi_{m,n}}\psi_{m+1,n} + J_y\psi_{m,n-1} + J_y\psi_{m,n+1}\Big), \tag{4}$$

where $\phi_{m,n} = \mathbf{q}\cdot\mathbf{R}_{m,n} = q_x ma + q_y na$. Note that the tunneling along y does not yield a phase because there is no tilt in the y direction; the tunneling amplitude along y depends on the depth of the grating, as illustrated in figure 1(d) with blue circles.

In order to demonstrate that the propagation of light in the continuous 2D potential $\delta n(x, y, z)$ is indeed equivalent to the dynamics of equation (4), we compare propagation in the discrete model (4), with that of the continuous equation (1). The lattice parameters are $\delta n_{\mathrm{L0}} = 4 \times 10^{-4}$, $a = 13$ μm; the tilt is given by $\eta = 0.1\delta n_{\mathrm{L0}}/a$; the grating is defined by $\delta n_{\mathrm{G0}} = 0.17\delta n_{\mathrm{L0}}$ and $q_x = -q_y = \pi/a$, which yields $\phi_{m,n} = (m - n)\pi$, and κ is chosen to yield resonant tunneling. The discrete lattice which corresponds to this choice of phases is illustrated in figure 2(a). It has two bands, $\beta = \pm 2\sqrt{K_x^2 \sin^2(k_x a) + J_y^2 \cos^2(k_y a)}$ (β is the propagation constant), touching at two 2D Dirac points at $(k_x, k_y) = (0, \pm\pi/2a)$ in the Brillouin zone [44], as depicted in figure 2(b). Suppose that the incoming beam at $z = 0$, excites the modes which are in the vicinity of these two Dirac points. Around these points, for a given $\hat{\mathbf{k}} = \mathbf{k}/k$, the group velocity, $\nabla_{\mathbf{k}}\beta(k_x, k_y)$, is constant. Thus, the beam will undergo conical diffraction, which has been thoroughly addressed with Dirac points in honeycomb optical lattices [27]. To demonstrate this effect, we consider the propagation of a beam with the

initial profile given by $\psi(x, y, 0) = \sqrt{I}\cos(y\pi/2a)\exp(-(x/3a)^2 - (y/3a)^2)$ in the 2D potential $\delta n(x, y, z)$ (the cosine term ensures that we excite modes close to the two Dirac points). In figure 2(c) we show this beam after propagation for $z = 162$ mm. The two concentric rings are a clear evidence of conical diffraction [27, 30]. We also compare this with the propagation in the discrete model (4), with tunneling phases plotted in figure 2(a); $K_x = 0.11\,\mathrm{mm}^{-1}, J_y = 0.14\,\mathrm{mm}^{-1}$. The results of the propagation in the discrete model are shown in figure 2(d). It is evident that for our choice of the tilt and the grating, we have effectively realized the lattice plotted in 2(a). This is in fact a realization of the Harper–Hofstadter Hamiltonian for $\alpha = 1/2$, where α is the flux per plaquette in units of the flux quantum [34, 35].

2.3. Proposal for experimental realization

For the experimental implementation of the scheme, we propose the so-called optical induction technique in photosensitive materials, which can be implemented in photorefractives [22–26]. In these systems, both the lattice $\delta n_{\mathrm{L}}(x, y)$ and the grating potential $\delta n_{\mathrm{G}}(x, y, z)$ can be obtained in a straightforward fashion by using interference of plane waves in the medium [26]. The lattice constant a, the grating parameter $\mathbf{q}$, and hence the hopping phase $\phi_{m,n} = \mathbf{q} \cdot \mathbf{R}_{m,n}$, are tunable by changing the angle between the interfering beams. This could enable manipulation of the phases of the tunneling matrix elements in real time [23].

The most challenging part of the implementation appears to be creation of the linear tilt potential. To observe the conical diffraction effects, one needs a linear gradient over the ~20 lattice sites, which implies a total index tilt $\Delta n = 20\eta a \sim 20 \times 0.1\delta n_{L0} \sim 8 \times 10^{-4}$. In principle, the linear tilt could be achieved by using a spatial light modulator. Another possibility which could create a linear tilt is to use crystals with linear dependence of the index of refraction on temperature, and a temperature gradient across the crystal [46].

However, it should be emphasized that if one uses a superlattice for δn_{L}, rather than the linear tilt potential, as in [33] for ultracold atomic gases, the grating assisted tunneling scheme proposed here would yield *staggered* synthetic magnetic fields for photons. The achievement of such staggered fields should be possible with optically induced lattices proposed here.

2.4. On the phase between the lattice and the grating

Before closing, we emphasize that the spatial phase between the periodic lattice potential δn_{L} and the grating δn_{G} is a relevant parameter. This point has recently been examined in detail in the context of ultracold atoms [45]. To translate it to our system, suppose that in our 1D system, we shift the grating along the x-direction, such that $\delta n_{\mathrm{G}} = \delta n_{\mathrm{G0}} \cos^2((q_x x - \kappa z + \xi)/2)$. This simply shifts the phases in the discrete lattice (shown in figure 1(c)) such that ϕ_m is replaced by $\phi_m + \xi$, which moves the 1D Dirac point in k_x-space by $\Delta k_x = \xi/a$. We have numerically verified that this indeed happens.

3. Conclusion

In conclusion, we have proposed the grating assisted tunneling scheme for tunable synthetic magnetic fields in optically induced one- and two-dimensional dielectric photonic lattices. As a signature of the synthetic magnetic fields and the Dirac points that these lattices possess in k-space, we have demonstrated conical diffraction patterns (shown in figures 1(c) and 2(a)). The excellent agreement between our results for light propagation in realistic (continuous) systems and the evolution in the corresponding discrete models, clearly confirms that the 2D dielectric photonic lattice with grating assisted tunneling constitutes the realization of the Harper–Hofstadter Hamiltonian. We envision that this approach can open the way for other studies of light propagation in tailored dielectric structures (including nonlinear propagation, solitons, instabilities and the creation of synthetic dimensions [47]) being mapped on intriguing discrete models with complex tunneling matrix elements and synthetic magnetic fields.

Acknowledgments

This work was supported by the Unity through Knowledge Fund (UKF Grant No 5/13). Work by MS (analysis and proof-reading of the manuscript) was supported as a part of S3TEC, and EFRC, funded by U S DOE, under Award Number DE-SC0001299 / DE-FG02-09ER46577. This work was also supported in part by the U S Army Research Laboratory and the U S Army Research Office through the Institute for Soldier Nanotechnologies, under Contract No W911NF-13-D-0001. We are grateful to Colin J Kennedy, Wolfgang Ketterle, Ling Lu and Mordechai Segev for useful conversations.

References

[1] Haldane F D M and Raghu S 2008 Possible realization of directional optical waveguides in photonic crystals with broken time-reversal symmetry *Phys. Rev. Lett.* **100** 013904
[2] Raghu S and Haldane F D M 2008 Analogs of quantum-Hall-effect edge states in photonic crystals *Phys. Rev.* A **78** 033834
[3] Wang Z, Chong Y, Joannopoulos J D and Soljačić M 2008 Reflection-free one-way edge modes in a gyromagnetic photonic crystal *Phys. Rev. Lett.* **100** 013905
[4] Wang Z, Chong Y, Joannopoulos J D and Soljačić M 2009 Observation of unidirectional backscattering-immune topological electromagnetic states *Nature* **461** 772
[5] Rechstman M C, Zeuner J M, Plotnik Y, Lumer Y, Podolsky D, Dreisow F, Nolte S, Segev M and Szameit A 2013 Photonic Floquet topological insulators *Nature* **496** 196
[6] Hafezi M, Mittal S, Fan J, Migdall A and Taylor J M 2013 Imaging topological edge states in silicon photonics *Nat. Photonics* **7** 1001
[7] Hafezi M, Demler E A, Lukin M D and Taylor J M 2011 Robust optical delay lines with topological protection *Nat. Phys.* **7** 907
[8] Umucalilar R O and Carusotto I 2011 Artificial gauge field for photons in coupled cavity arrays *Phys. Rev.* A **84** 043804
[9] Fang K, Yu Z and Fan S 2012 Realizing effective magnetic field for photons by controlling the phase of dynamic modulation *Nat. Photonics* **6** 782
[10] Rechtsman M C, Zeuner J M, Tünnermann A, Nolte S, Segev M and Szameit A 2013 Strain-induced pseudomagnetic field and photonic Landau levels in dielectric structures *Nat. Photonics* **7** 153
[11] Zeuner J M, Efremidis N K, Keil R, Dreisow F, Christodoulides D N, Tunnermann A, Nolte S and Szameit A 2012 Optical analogues for massless Dirac particles and conical diffraction in one-dimension *Phys.Rev. Lett.* **109** 023602
[12] Manela O, Segev M, Christodoulides D N and Kip D 2010 Hofstadter butterflies in nonlinear Harper lattices, and their optical realizations *New J. Phys.* **12** 053017
[13] Kraus Y, Lahini Y, Ringel Z, Verbin M and Zilberberg O 2012 Topological States and Adiabatic Pumping in Quasicrystals *Phys. Rev. Lett.* **109** 106402
[14] Longhi S 2013 Effective magnetic fields for photons in waveguide and coupled resonator lattices *Opt. Lett.* **38** 18
[15] Khanikaev A B, Mousavi S H, Tse W-K, Kargarian M, MacDonald A H and Shvets G 2013 Photonic topological insulators *Nat. Mater.* **12** 233
[16] Lu L, Fu L, Joannopoulos J D and Soljačić M 2013 Weyl points and line nodes in gyroid photonic crystals *Nat. Photonics* **7** 294
[17] Mukherjee S, Spracklen A, Choudhury D, Goldman N, Öhberg P, Andersson E and Thomson R R 2015 Modulation-assisted tunneling in laser-fabricated photonic Wannier–Stark ladders *New J. Phys.* **17** 115002
[18] Lu L, Joannopoulos J D and Soljačić M 2014 Topological photonics *Nat. Photonics* **8** 821
[19] Dalibard J, Gerbier F, Juzeliunas G and Öhberg P 2011 Coll.: artificial gauge potentials for neutral atoms *Rev. Mod. Phys.* **83** 1523
[20] Goldman N, Juzeliunas G, Ohberg P and Spielman I B 2014 Light-induced gauge fields for ultracold atoms *Rep. Prog. Phys.* **77** 126401
[21] Hasan M Z and Kane C L 2010 Colloquium: Topological insulators *Rev. Mod. Phys.* **82** 3045
[22] Efremidis N K, Sears S, Christodoulides D N, Fleischer J W and Segev M 2002 Discrete solitons in photorefractive optically induced photonic lattices *Phys. Rev.* E **66** 046602
[23] Fleischer J W, Carmon T, Segev M, Efremidis N K and Christodoulides D N 2003 Observation of discrete solitons in optically induced real time waveguide arrays *Phys. Rev. Lett.* **90** 023902
[24] Fleischer J W, Segev M, Efremidis N K and Christodoulides D N 2003 Observation of two-dimensional discrete solitons in optically induced nonlinear photonic lattices *Nature* **422** 147
[25] Neshev D, Ostrovskaya E, Kivshar Y and Krolikowski W 2003 Spatial solitons in optically induced gratings *Opt. Lett.* **28** 710
[26] Fleischer J W, Bartal G, Cohen O, Schwartz T, Manela O, Freedman B, Segev M, Buljan H and Efremidis N K 2005 Spatial photonics in nonlinear waveguide arrays *Opt. Express* **13** 1780
[27] Peleg O, Bartal G, Freedman B, Manela O, Segev M and Christodoulides D N 2007 Conical diffraction and gap solitons in Honeycomb photonic lattices *Phys. Rev. Lett.* **98** 103901
[28] Guinea F, Katsnelson M I and Geim A K 2010 Energy gaps and a zero-field quantum Hall effect in graphene by strain engineering *Nat. Phys.* **6** 30
[29] Szameit A, Kartashov Y V, Dreisow F, Heinrich M, Pertsch T, Nolte S, Tünnermann A, Vysloukh V A, Lederer F and Torner L 2009 Inhibition of light tunneling in waveguide arrays *Phys. Rev. Lett.* **102** 153901
[30] Berry M V 2004 Conical diffraction asymptotics: fine structure of Poggendorff rings and axial spike *J. Opt. A. Pure Appl. Opt.* **6** 289
[31] Harper P G 1955 Single band motion of conduction electrons in a uniform magnetic field *Proc. Phys. Soc. London* A **68** 874
[32] Hofstadter D R 1976 Energy levels and wave functions of Bloch electrons in rational and irrational magnetic fields *Phys. Rev.* B **14** 2239
[33] Aidelsburger M, Atala M, Nascimbene S, Trotzky S, Chen Y-A and Bloch I 2011 Experimental realization of strong effective magnetic fields in an optical lattice *Phys. Rev. Lett.* **107** 255301
[34] Miyake H, Siviloglou G A, Kennedy C J, Cody Burton W and Ketterle W 2013 Realizing the Harper Hamiltonian with laser-assisted tunneling in optical lattices *Phys. Rev. Lett.* **111** 185302
[35] Aidelsburger M, Atala M, Lohse M, Barreiro J T, Paredes B and Bloch I 2013 Realization of the Hofstadter Hamiltonian with ultracold atoms in optical lattices *Phys. Rev. Lett.* **111** 185301
[36] Jaksch D and Zoller P 2003 Creation of effective magnetic fields in optical lattices: the Hofstadter butterfly for cold neutral atoms *New J. Phys.* **5** 56
[37] Kolovsky A R 2011 Creating artificial magnetic fields for cold atoms by photon-assisted tunneling *Europhys. Lett.* **93** 003
[38] Madison K W, Chevy F, Wohlleben W and Dalibard J 2000 Vortex Formation in a Stirred Bose–Einstein Condensate *Phys. Rev. Lett.* **84** 806
[39] Abo-Shaeer J R, Raman C, Vogels J M and Ketterle W 2001 Observation of vortex lattices in Bose–Einstein condensates *Science* **292** 476
[40] Lin Y-J, Compton R L, Jiménez-García K, Porto J V and Spielman I B 2009 Synthetic magnetic fields for ultracold neutral atoms *Nature* **462** 628
[41] Struck J, Ölschläger C, Weinberg M, Hauke P, Simonet J, Eckardt A, Lewenstein M, Sengstock K and Windpassinger P 2012 Tunable gauge potential for neutral and spinless particles in driven optical lattices *Phys. Rev. Lett.* **108** 225304
[42] Aidelsburger M, Lohse M, Schweizer C, Atala M, Barreiro J T, Nascimbène S, Cooper N R, Bloch I and Goldman N 2015 Measuring the Chern number of Hofstadter bands with ultracold bosonic atoms *Nat. Phys.* **11** 162–6
[43] Christodoulides D N, Lederer F and Silberberg Y 2003 Discretizing light behavior in linear and nonlinear waveguide lattices *Nature* **424** 817

[44] Miyake H 2013 Probing and preparing novel states of quantum degenerate rubidium atoms in optical lattices *PhD Thesis* Massachusetts Institute of Technology
[45] Tarallo M G, Alberti A, Poli N, Chiofalo M L, Wang F-Y and Tino G M 2012 Delocalization-enhanced Bloch oscillations and driven resonant tunneling in optical lattices for precision force measurements *Phys. Rev.* A **86** 033615
[46] Alfassi B, Rotschild C, Manela O, Segev M and Christodoulides D N 2006 Boundary force effects exerted on solitons in highly nonlocal nonlinear media *Opt. Lett.* **32** 154
[47] Jukić D and Buljan H 2013 Four-dimensional photonic lattices and discrete tesseract solitons *Phys. Rev.* A **87** 013814